In considering the excitation functions from this point of view, it is helpful to have available an energy level scheme for the isotopes involved. Such a scheme has been presented in Fig. 6. It was adapted from the values given in the very comprehensive review of energy levels of light nuclei given by Ajzenberg and Lauritsen.[1] All the indicated levels are plotted at energies relative to the ground state energy of Be^9 plus a deuteron. The energies indicated are those in the center-of-mass system.

A plot of the two excitation functions drawn to the same energy scale has been included in the figure.

ACKNOWLEDGMENTS

The authors are very anxious to acknowledge the great assistance given by the Argonne National Laboratory and the crew of its cyclotron is providing the bombardments. They wish to thank Mr. Melvin Fielding for operation of the 8-Mev Chicago cyclotron, Dr. James R. Arnold for the use of his scintillation sysectrometer and Dr. Kay K. Chenye for the preparation of special foils. Finally, they wish to thank the U. S. Air Force, Office of Scientific Research and Development, for financial support.

PHYSICAL REVIEW VOLUME 100, NUMBER 3 NOVEMBER 1, 1955

Electric Excitation of Certain Rare-Earth Nuclei by Protons*

HANS MARK† AND GEORGE T. PAULISSEN
Department of Physics and Laboratory for Nuclear Science, Massachusetts Institute of Technology, Cambridge, Massachusetts
(Received July 28, 1955)

Sixteen energy levels have been observed in thirteen isotopes of samarium, europium, gadolinium, and terbium. Electric quadrupole transition probabilities have been determined for some of these energy levels from the measured electric excitation cross sections. For the even-A isotopes of Gd, the properties of the low-lying energy levels are in good agreement with the expectations of the "strong coupling" rotational model. The first energy levels in the even isotopes of samarium show the sharp break in the position of the first excited level which has recently been pointed out by Scharff-Goldhaber. In general, the results are in good qualitative agreement with the predictions of the collective model; however, the moments of inertia for the rotational levels observed in this region are substantially larger than those expected from the intrinsic deformations obtained from the radiative transition probabilities.

I. INTRODUCTION

SINCE the discovery of electric excitation nearly three years ago,[1,2] a large amount of information concerning nuclear energy level structure has been collected by means of this process. Over one hundred isotopes, ranging from F^{19} to U^{238}, have been bombarded by α particles (see publications of G. M. Temmer and N. P. Heydenburg; Sherr, Li, and Christy; and Torben Huus and collaborators) or protons (see publications of Eisinger, Cook, and Class; R. M. Williamson and W. I. Goldburg; P. H. Stelson and F. K. McGowan; Simmons, Van Patter, Famularo, and Stuart; Torben Huus and collaborators; and McClelland, Mark, and Goodman) and in most isotopes, the existence of one or more energy levels has been established. Most workers have observed the γ rays emitted after the excitation of the nucleus while others (see Torben Huus and collaborators and W. I. Goldburg and R. M. Williamson) have detected the internal conversion electrons which, in most cases, also follow the nuclear excitation. For some nuclei, the angular distribution of γ rays following electric excitation has also been determined (see Eisinger, Cook and Class; W. I. Goldburg and R. M. Williamson; P. H. Stelson and F. K. McGowan; and Simmons *et al.*).

An electric excitation event is said to occur when an energetic charged particle passes by a nucleus and exchanges some of its kinetic energy with the nucleus through the agency of the electric field existing between the projectile and the nucleus. In the vast majority of the cases observed so far it is the quadrupole term of this field which gives rise to the excitation but it is of course possible, in principle, to excite energy levels having other multipole orders as well.[3,4] The energy levels of the nucleus being bombarded are then studied by observing the energies of the γ rays which are emitted upon the decay of the excited nucleus. The number of γ rays per charged particle (i.e., the electric excitation cross section) is related to the radiative transition probability of the energy level under investigation. Since large radiative transition probabilities give rise to large electric excitation cross sections, the process has been particularly useful for the study of the

* Supported in part by the joint program of the Office of Naval Research and the U. S. Atomic Energy Commission.
† Now at the Department of Physics, University of California, Berkeley, California.
[1] C. L. McClelland and Clark Goodman, Phys. Rev. **91**, 760 (1953).
[2] T. Huus and C. Zupančič, Kgl. Danske Videnskab. Selskab, Mat.-fys. Medd. **28**, No. 1 (1953).
[3] Sherr, Li, and Christy, Phys. Rev. **94**, 1076 (1954).
[4] G. M. Temmer and N. P. Heydenburg, Phys. Rev. **94**, 1252 (1954).

so-called "collective" transitions in nuclei. The great abundance of these "collective" levels throughout the periodic table has served as an excellent qualitative confirmation of the validity of Aage Bohr's "collective" model of nuclear structure.[5]

In general, there is remarkably good agreement among the experimental workers in the field regarding the position of energy levels in the many isotopes which have been studied. However, quite serious discrepancies exist in the measured electric excitation cross sections and hence in the measured values of the radiative transition probabilities. These discrepancies are caused by the difficulties in measuring absolute γ-ray yields with presently available techniques and will be discussed in detail in the following section. It has been suggested[6] that many of the existing uncertainties in the measured cross sections (such as uncertainties in stopping power, detector efficiency, etc.) would disappear if the ratio of elastically to inelastically scattered particles from a given level were measured rather than the number of γ rays (or internal conversion electrons) which are emitted per bombarding particle. In such experiments, any uncertainties, due to internal conversion, in the radiative transition probabilities calculated from the cross sections would also be absent. Experiments of this type have recently been performed[7] at the Massachusetts Institute of Technology using the new high-resolution, charged-particle spectrograph of the MIT-ONR generator group with very promising results.

II. EXPERIMENTAL METHODS

The experimental procedures used in the series of measurements to be described are substantially the same as those which have been used previously[8,9] in similar experiments. Some changes have been made which were designed to improve the γ-ray yield measurements. The basic problem of measuring the number of γ rays per proton can be conveniently divided into three parts: the determination of the proton beam current, the determination of the attenuation suffered by the γ rays as they travel from the target to the detector, and the determination of the efficiency of the detector for γ rays of a given energy for the experimental geometry used. The proton beam current was measured with a standard beam current integrator which consists of a condenser in parallel with a relay which closes whenever the voltage across the condenser reaches a certain point. This instrument was calibrated with a standard battery to within 2%. It is improbable, however, that the actual beam current is known this accurately since there is considerable secondary electron emission when targets are bombarded with high-energy protons. Several tests with targets at different positive voltages were made to estimate the size of this effect, and as a result of these studies, the estimated error in the beam current is of the order of 10%.

The attenuation of the γ rays between the target and the detector arises from self-absorption in the target, absorption in the aluminum target holder tube, absorption in the aluminum housing and the magnesium oxide layer of the crystal, and absorption in the tin sheets which were used to reduce the background of characteristic x-rays from each target. All of these effects except the last are reasonably small even for γ rays of energies of the order of 80 kev ($\sim$20% attenuation), and therefore the expected attenuation was calculated using published values of absorption coefficients.[10] The attenuation of the γ rays in the tin absorbers is quite large ($\sim$60%) for the lowest energy γ rays, and hence the absorption in the tin was determined experimentally by measuring the attenuation for a given γ ray as a function of absorber thickness. The error in γ-ray yield per proton due to attenuation of the γ rays will be a function of γ-ray energy. The smallest errors ($\sim$5%) will occur for the γ rays with the highest energies (i.e., smallest attenuation) and larger errors ($\sim$15%) are expected for the lowest energy γ rays.

By far the most troublesome problem encountered in the determination of absolute γ-ray yields is the determination of the absolute efficiency of the detector. In all cases, the γ-ray intensity was determined by graphical integration of the photopeak in the pulse-height spectrum (see Figs. 2, 3, 4, 5, 6, and 7). The proton bremsstrahlung[11,12] background was subtracted out experimentally. The error in the yield due to background subtraction is roughly 5%. Since the area of the photo-peak is used as a measure of the γ-ray intensity, the efficiency of the crystal for the production of pulses in the photo-peak must be determined. For γ rays with energies below 100 kev, large (2 in.$\times$2 in.) NaI crystals are substantially 100% efficient detectors—that is, almost every γ ray which strikes the face of the crystal gives rise to a pulse in the photopeak. For higher energy γ rays this is no longer the case, and therefore the efficiency must either be calculated theoretically or measured. Pulses in the photopeak arise from two sources: a γ ray may be absorbed by an atom emitting a photo-electron which carries off the entire energy of the γ ray; or a γ ray may undergo one or more Compton collisions with almost free electrons in the crystal, and then the final degraded photon ultimately is absorbed in a photoelectric event. Both of these events give rise to pulses in tbe photopeak and hence both must be included in a theoretical calculation of the efficiency.

[5] A. Bohr and B. R. Mottelson, Kgl. Danske Videnskab. Selskab, Mat.-fys. Medd. **27**, No. 16 (1953).
[6] H. Mark, Phys. Rev. **94**, 1436(A) (1954).
[7] W. W. Buechner and C. K. Bockelman (private communication).
[8] McClelland, Mark, and Goodman, Phys. Rev. **97**, 1191 (1955).
[9] Mark, McClelland, and Goodman, Phys. Rev. **98**, 1245 (1955).
[10] C. M. Davisson and R. D. Evans, Revs. Modern Phys. **24**, 79 (1952).
[11] C. Zupančič and T. Huus, Phys. Rev. **94**, 205 (1954).
[12] Mark, McClelland, and Goodman, Phys. Rev. **98**, 279(A) (1955).

Meader, Muller, and Wintersteiger[13] have made extensive calculations of NaI photopeak efficiency and their results have been used to interpolate the photopeak efficiency curve between experimental points.

The photopeak efficiency of the crystal was determined for annihilation radiation (510 kev) from a Na^{22} source by a γ-γ coincidence experiment and for 279-kev γ rays from a Hg^{203} source by a β-γ coincidence experiment, using the equipment shown in Fig. 1. For the β-γ coincidence experiment one of the γ counters was replaced by a pilot B plastic scintillator 0.05 in. thick mounted on a du Mont 6292 photomultiplier tube. This counter was sensitive only to the β particles emitted by the source. In both cases measurements were made for several different geometries including the one actually used in the experiment. For the annihilation radiation, counter B was set so that only the photopeak pulses were large enough to trip the coincidence circuit. Because of the back-to-back correlation of the annihilation quanta, the photopeak efficiency of counter B is then just the ratio of the number of counts in the photopeak observed at the coincidence output to the number of counts in the photopeak at the analyzer output. For the geometry used in the electric excitation experiments (i.e., crystal faces $\frac{5}{16}$ in. from the target and perpendicular to proton beam) this number is 0.25 ± 0.02. Assuming that the effective range of a 510-kev photon in the crystal is 0.9 in., the photopeak efficiency for the geometry used in these experiments can be obtained by multiplying 0.25 by the effective solid angle subtended by the counter B at the target. The photopeak efficiency for the experimental geometry determined in this manner is 0.033. The error in this number may be as large as 30% or more because of the uncertainty in determining the effective solid angle. In the case of the 279-kev radiation from Hg^{203}, counter B was again set so that only photopulses of the γ rays tripped the coincidence circuit and counter A was replaced by the electron counter. Since the β and γ rays from the source are essentially directionally uncorrelated, the ratio of counts at the coincidence output to those at the analyzer output is a direct measure of the photopeak efficiency for the experimental geometry. For the experimental geometry used in the cross-section measurements, this ratio was 0.15. It should be pointed out, however, that this result may also be in error by 30% or more because of scattered low-energy electrons from the source and because the 279-kev γ ray is quite highly internally converted[14] giving rise to electrons which are not accompanied by γ rays. (It was possible with the pilot B scintillator to observe both the K and L conversion lines from the 279-kev transition. The resolution was roughly 35%. The actual coincidence ratios were taken at an energy near the maximum of the β spectrum—between 50 and 80 kev. The background from the internal conversion lines and from scattered electrons at this energy was unfortunately still considerable.) In view of the many uncertainties in the theoretical interpolations and in the calibration measurements themselves, the errors in the γ-ray yield are of the order of 50% due to uncertainties in detector calibration alone. The error from this source will of course be a function of γ-ray energy with the largest errors occurring for the γ rays with the highest energy. However, as has been pointed out, the uncertainties in the attenuation of the γ rays behave in the opposite manner with the largest errors occurring for the lowest-energy γ rays. It is probable, therefore, that the absolute error in the number of γ rays per proton stays reasonably constant as a function of γ-ray energy.

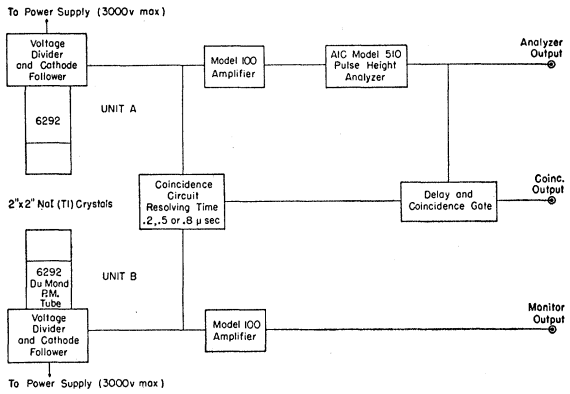

FIG. 1. Experimental equipment. The equipment used for the detection of the γ rays is shown in this figure. A signal appears at the coincidence output whenever a pulse in crystal B is in coincidence with a pulse in crystal A which is within the window of the single-channel analyzer. The coincidence circuit is not activated by pulses from the counters which are below a certain voltage, and hence the system possesses a cut-off point below which it will not work. The position of the cut-off point can be adjusted by varying the high voltage across unit B. The pulses observed at the analyzer output represent the pulse spectrum in unit A while the monitor output registers all pulses in unit B.

The experimental geometry employed is also somewhat different from that which has been described previously.[8] The crystals were placed, one on each side of the target holder, with their axes perpendicular to the proton beam and their faces $\frac{5}{16}$ in. from the target. The beam was focused on the target on a spot roughly 0.5 mm square. In this way, errors in the total γ yield due to the angular distribution of the emitted γ rays are reduced to less than 5%. The aluminum target holder tube was 0.5 in. in diameter and the walls were $\frac{1}{16}$ in. thick. The targets in all cases were made of the metallic oxide powder ($\sim$30 mg) compressed on a small ($\frac{1}{4}$-in. diameter) aluminum plug which was held in position between the crystals on a thin brass rod. The inside of the holder tube was lined with 0.002-in. tin sheet to eliminate background radiations arising from scattered protons striking the aluminum tube.

There are two reasons for using both crystals in coincidence during the electric excitation experiments.

[13] Maeder, Muller, and Wintersteiger, Helv. Phys. Acta **27**, 3 (1954).
[14] D. Saxon, Phys. Rev. **74**, 849 (1948).

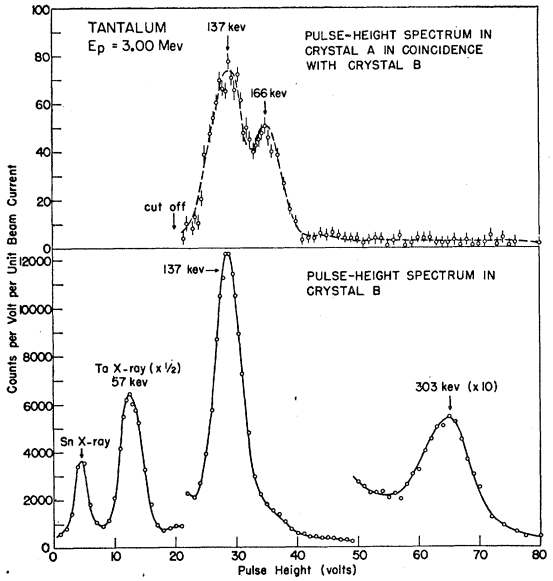

FIG. 2. Pulse-height spectrum observed from tantalum target during bombardment with 3-Mev protons. The lower panel shows the spectrum observed at the analyzer output and the upper panel shows the spectrum at the coincidence output. The peak corresponding to the tin x-ray seen in the singles spectrum comes from fluorescence radiation of the tin absorber between the target and the detector. The voltage across counter B is adjusted so that the coincidence circuit is not tripped by the x-ray pulses and therefore they do not contribute to the random background. The 137-kev peak observed in the coincidence spectrum is slightly larger than the 166-kev peak because of the large random background at this point due to the excitation of the 137-kev level alone.

One is to observe cascade transitions in odd A nuclei where it is often possible to excite the first two energy levels. Figure 2 shows the pulse-height spectrum obtained when a thick tantalum metal target is bombarded with 3-Mev protons. The unbroken curve shows the spectrum obtained in one crystal in coincidence with pulses in the other. In the singles spectrum, peaks corresponding to energies of 137 and 303 kev are observed. These peaks are caused by γ rays coming from the decay of the first two energy levels in this isotope. The coincidence spectrum shows peaks at 166 kev and 137 kev which come from the cascade decay of the 303-kev level and are therefore in coincidence. From such measurements it is possible to determine the ratio of the number of cascade to crossover γ rays for the second energy level. Such measurements have been made for a number of odd A nuclei[15] and are presently being extended. The other reason for using the coincidence spectrometer in the electric excitation experiments is that it aids in the identification of impurity γ rays. A γ ray at 510 kev is observed from all oxide targets which is accompanied by a high coincidence counting rate characteristic of annihilation radiation (see Fig. 3). It is very probable that this γ ray arises from annihilation radiation emitted[16] in the decay of F^{17} which is produced in the target by the reaction $O^{16}(p,\gamma)F^{17}$. The continuous coincidence background observed from oxide targets is of the order of 5 times larger than that observed from metallic targets which indicates the presence of high-energy capture γ rays emitted in cascade transitions between highly excited states in F^{17}.

In all cases, the yield of γ rays was measured from targets which were thick to 3-Mev protons. The energy calibration of the scintillation spectrometer was carried out by using the methods which have been described in reference 9. The γ-ray energies quoted in column 2 of Table I are considered accurate to 5% except for some special cases which will be discussed in the next section. Column 5 in the table of results shows the

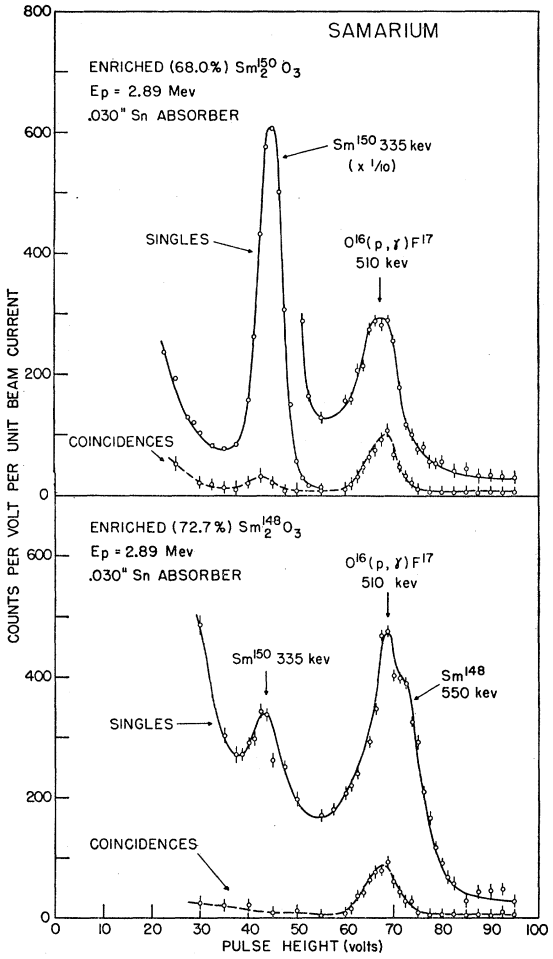

FIG. 3. Pulse-height spectra observed from $(Sm^{148})_2O_3$ and $(Sm^{150})_2O_3$ targets during bombardment with 2.89-Mev protons. This figure shows the peaks corresponding to γ rays of 335 kev and 550 kev which arise from the excitation of energy levels in Sm^{150} and Sm^{148} respectively. The peak at 510 kev is due to annihilation radiation which probably comes from the decay of F^{17} produced in the oxide target by the reaction $O^{16}(p,\gamma)F^{17}$.

[15] H. Mark and G. Paulissen, Phys. Rev. **99**, 1654 (A) (1955).

[16] F. Ajzenberg and T. Lauritsen, Revs. Modern Phys. **27**, 77 (1955).

TABLE I. The experimental results are summarized in this table. Column 4 lists the proton energies at which the cross section measurements were made. The values of $B(E2)$ listed in column 8 are the reduced transition probabilities for the excitation of the level. The values of Q_0 (energy) listed in column 10 are calculated from Eq. (2) in reference 8 assuming $R_0=1.44A^{1/3}\times10^{-13}$ cm.

Nuclide	E_γ(kev)	$I_0\rightarrow I$	E_p(Mev)	$N\gamma$/proton (10^{-9})	$B(E2)/(\alpha_T+1)$ (10^{-48} cm^4)	α_T	$B(E2)$ (10^{-48} cm^4)	Q_0(cross section (10^{-24} cm^2)	Q_0(energy) (10^{-24} cm^2)
Sm^{148}	550[a]	0→2	2.88	4.8	0.74	10^{-3}	0.74	2.7	7.39
Sm^{150}	335	0→2	2.88	13.9	0.51	0.03	0.52	2.3	9.45
Sm^{152}	125	0→2	2.88	53.9	0.43	1.6	1.1	3.3	15.4
Sm^{154}	84	0→2	2.88	41.2	0.27	6.3	2.0	4.5	18.8
Eu^{151}	300	5/2→?	2.88	2.0	...	...	...	...	...
Eu^{153}	85	5/2→7/2	2.88	15.8	0.20[b]	4.0	1.0	5.0	21.8
	115	...	2.88	2.5	...	...	...	...	...
	200	5/2→9/2	2.88	6.5	0.14	0.05	0.15	...	...
Gd^{154}	123[c]	0→2	1.88	8.8	1.0	1.6	2.6	5.1	16.0
Gd^{155}	140[a]	7/2→?	2.88	...	...	...	...	...	...
Gd^{156}	89	0→2	1.88	2.2	0.74	5.7	5.0	7.1	18.8
Gd^{157}	127[a]	7/2→?	2.88	...	...	...	...	...	...
Gd^{158}	80	0→2	1.88	2.4	0.63	8.6	6.0	7.7	19.8
Gd^{160}	76	0→2	1.88	3.0	0.73	12.0	9.5	9.7	20.2
Tb^{159}	77	3/2→?	2.88	...	...	...	...	...	...
	167[d]	3/2→?	2.88	...	...	...	...	...	...

[a] Error ±10%.
[b] Calculated assuming no contribution from cascade.
[c] Composite line.
[d] Probable impurity line.

number of γ rays per proton obtained from each target. The absolute error in this number from all the sources discussed in this section is of the order of 75% and in some special cases, which will be discussed in the next section, may be even larger. However, the relative errors between yields from different isotopes of the same element are much smaller (of the order of 15%) since many of the factors which contribute to the large absolute error tend to cancel out. The conversion of the measured yield to the electric excitation cross section will be discussed in the final section.

III. EXPERIMENTAL RESULTS

Sixteen γ rays have been observed in thirteen isotopes of samarium, europium, gadolinium, and terbium. Many of these γ rays have already been observed by other workers following the β decay of unstable isotopes in the same region of the periodic table and all of them have also been observed by Temmer and Heydenburg[17] by electric excitation with α particles and by Huus, Bjerregard, and Elbek[18] who have studied the internal conversion electrons emitted from many of these materials upon bombardment with protons. (The authors are indebted to Dr. Temmer for sending us a preprint of his results prior to publication and also to Dr. Elbek who supplied us with a rough draft copy of his paper.) In most cases, the isotopic assignments of the γ rays were determined by bombarding samples of enriched isotopes. For those elements where enriched samples were not available, the most probable assignment was made on the basis of previously published work.

Sm^{148}

The pulse-height spectrum obtained when an enriched (72.7%) $(Sm^{148})_2O_3$ target is bombarded with 2.89-Mev protons is shown in the lower panel of Fig. 3. A γ ray at 550 kev is observed which comes from the excitation of an energy level in Sm^{148}. Unfortunately, the 510-kev annihilation radiation of roughly equal intensity from the $O^{16}(p,\gamma)F^{17}$ reaction partially obscures the 550-kev radiation. The upper panel of Fig. 3 shows the pulse-height spectrum obtained from an enriched $(Sm^{150})_2O_3$ target obtained under similar conditions. This target contained only 2.54% Sm^{148}, and therefore the peak at 510 kev in this spectrum is caused entirely by the annihilation radiation. The intensity and energy of the 550-kev line were estimated by subtracting the curve in the upper panel from the lower one. The errors in both the energy and the intensity of this γ ray are unusually large because of this background effect.

Sm^{150}

The upper panel in Fig. 3 shows the pulse-height spectrum obtained when an enriched (68.0%) $(Sm^{150})_2O_2$ target is bombarded with 2.89-Mev protons. The strong γ ray at 335 kev comes from the excitation of an energy level in Sm^{150} at about this energy (336.7 kev) which is also observed[19] following the β decay of Pm^{150}.

Sm^{152}

The pulse-height spectrum obtained when enriched (96.0%) $(Sm^{152})_2O_3$ is bombarded with 2.89-Mev protons is shown by the dashed curve in Fig. 4. A strong γ ray at 125 kev is observed which comes from the excitation of a level at this energy in Sm^{152} which is also observed[20] following the positron decay of Eu^{152}.

[17] G. M. Temmer and N. P. Heydenburg (private communication).
[18] Huus, Bjerregard, and Elbek, Kgl. Danske Videnskab. Selskab, Mat.-fys. Medd. (to be published).
[19] V. K. Fischer, Phys. Rev. **96**, 1549 (1954).
[20] Slattery, Lu, and Wiedenbeck, Phys. Rev. **96**, 465 (1954).

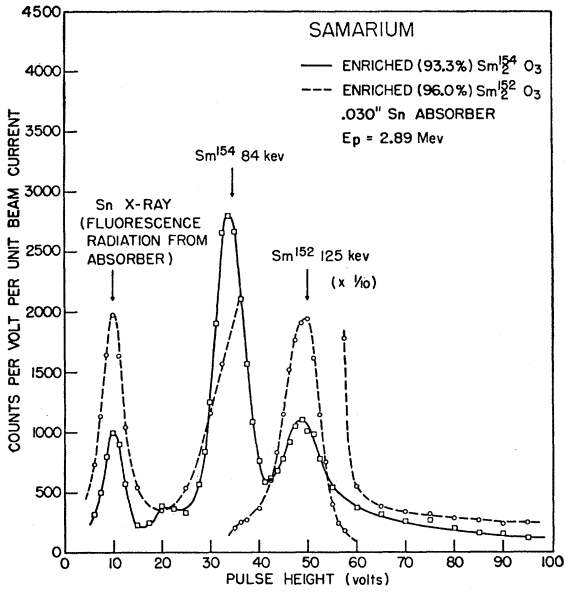

FIG. 4. Pulse-height spectra observed from $(Sm^{152})_2O_3$ and $(Sm^{154})_2O_3$ targets during bombardment with 2.89-Mev protons. This figure shows peaks corresponding to γ rays of 125 kev and 84 kev which arise from the excitation of energy levels in Sm^{152} and Sm^{154}, respectively.

Sm^{154}

The solid line in Fig. 4 shows the pulse-height spectrum when enriched (93.3%) $(Sm^{154})_2O_3$ is bombarded with 2.89-Mev protons. A γ ray at 84 kev is observed which comes from the excitation of a level in Sm^{154}. The peak at 125 kev observed in this spectrum comes from the 3.2% Sm^{152} present in this sample.

Eu^{151}

No enriched isotopes of europium were available for these experiments. Four γ rays (300 kev, 200 kev, 115 kev, and 85 kev) are observed when a natural Eu_2O_3 target is bombarded with protons. The γ ray at 300 kev has been tentatively assigned to the 47.8% abundant Eu^{151} by Temmer and Heydenburg.[17] This assignment is probably correct because no γ ray of this energy is observed[20] following the β decays of Gd^{153} and Sm^{153}.

Eu^{153}

The other three γ rays which are observed when the natural Eu_2O_3 is bombarded with 2.89-Mev protons are shown in the upper panel in Fig. 5. The three γ rays at 200 kev, 115 kev, and 85 kev probably arise from the excitation of the first two energy levels at 85 kev and 200 kev in 52.2% abundant Eu^{153}. There is some evidence that the 115-kev γ ray is always in coincidence with an 85-kev γ ray, indicating that the 115-kev γ ray arises from the cascade decay of the 200-kev level in this isotope. However, this scheme cannot be definitely established from our data because of the large coincidence background from oxide targets. Several γ rays of similar energies are observed[21] in the β decay of Sm^{153}; however, the level schemes proposed in references 21 and 22 are not in agreement with our data or the data of Temmer and Heydenburg.[17]

Gd^{154}

The pulse-height spectrum obtained when an enriched (33%) target of $(Gd^{154})_2O_3$ is bombarded with 2.89-Mev protons is shown by the dotted curve in Fig. 6.

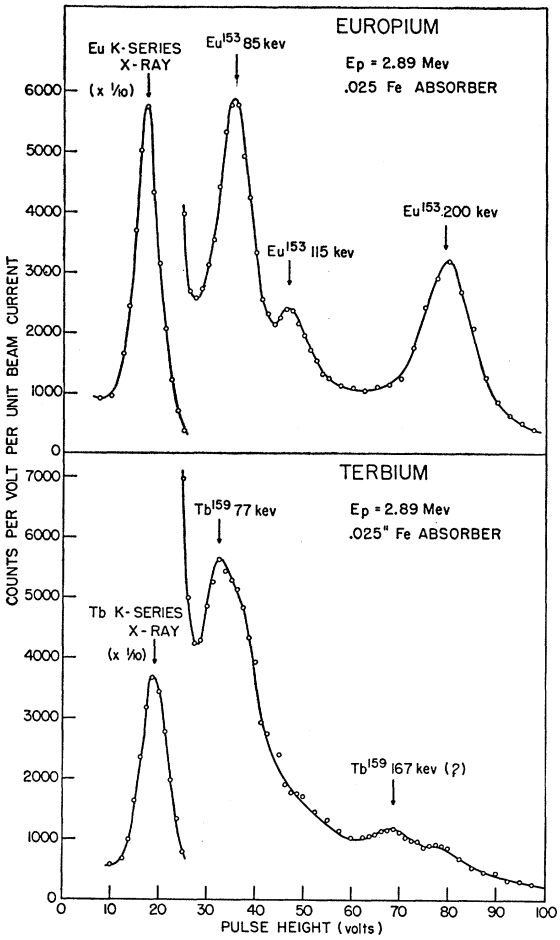

FIG. 5. Pulse-height spectra observed during the bombardment of Eu_2O_3 and Tb_2O_3 targets with 2.89-Mev protons. The peaks corresponding to γ rays at 85, 115, and 200 kev in the upper panel probably arise from the excitation of the first two rotational levels in Eu^{153}. This drawing is a good example of a rotational spectrum observed in an electric excitation process. There is some evidence that every 115-kev γ ray is always in coincidence with an 85-kev γ ray. A γ ray at 300 kev is observed from the europium targets which has roughly the intensity of the 200-kev peaks and probably arises from the excitation of a level in Eu^{151}. The terbium spectrum shown in the lower panel is not considered too reliable for reasons which are explained in the text.

[21] *Nuclear Data*, National Bureau of Standards Circular Report No. 499 (U. S. Government Printing Office, Washington, D. C., 1950).

[22] Cork, Leblanc, Nester, and Stumpf, Phys. Rev. 88, 685 (1952).

A strong γ ray at 123 kev is observed which is also seen[20] in the β decay of Eu^{154}. The small peak at 85 kev in this spectrum is caused by the presence of 16% of Gd^{156} in the sample.

$Gd^{155,157}$

The pulse-height spectrum obtained when natural Gd_2O_3 targets are bombarded with 2.89-Mev protons is shown by the unbroken curve in Fig. 6. The γ rays corresponding to the two peaks at ~127 and ~140 kev have been assigned by Temmer and Heydenburg[17] to energy levels in 15.7% abundant Gd^{157} and 14.7% abundant Gd^{155}, respectively. No cross-section measurements were made for these lines since their intensities are so low. The peak at 127 kev is certainly composite, with the 123-kev line in 2.15% abundant Gd^{154} contributing to the observed intensity.

Gd^{156}

Figure 7 shows the pulse-height spectrum obtained when enriched (80.22%) $(Gd^{156})_2O_3$ is bombarded with 1.71-Mev protons. A peak corresponding to a γ ray of 89 kev is observed which comes from the excitation of an energy level in this isotope.

Gd^{158}

The dotted curve in Fig. 7 shows the pulse-height spectrum when enriched (92.9%) $(Gd^{158})_2O_3$ targets are bombarded with 1.71-Mev protons. A peak is observed corresponding to a γ ray of 80 kev which comes from the excitation of an energy level in this isotope.

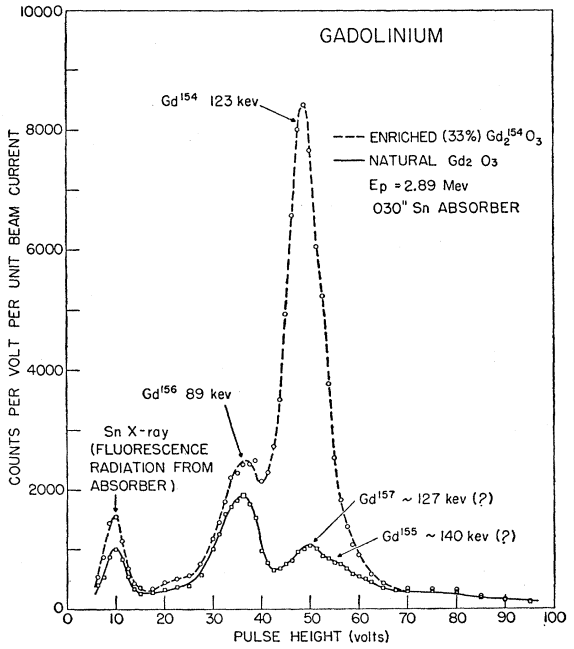

FIG. 6. Pulse-height spectra observed during the bombardment of enriched $(Gd^{154})_2O_3$ and natural Gd_2O_3 bombarded with 2.89-Mev protons. The strong peak corresponding to a γ ray at 123 kev is due to excitation of a level in Gd^{154} and the two bumps on the curve at about 127 and 140 kev are probably caused by the excitation of levels in Gd^{157} and Gd^{155}, respectively.

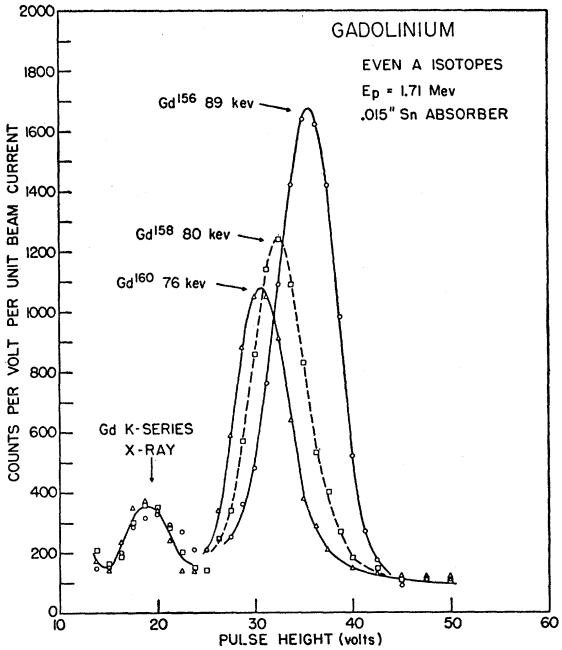

FIG. 7. Pulse-height spectra observed during the bombardment of $(Gd^{156})_2O_3$, $(Gd^{158})_2O_3$, and $(Gd^{160})_2O_3$ targets by 1.71-Mev protons. The peaks observed at 89, 80, and 76 kev arise from the excitation of energy levels in Gd^{156}, Gd^{158}, and Gd^{160}, respectively.

Gd^{160}

The pulse-height spectrum observed when an enriched (95.4%) $(Gd^{160})_2O_3$ target is bombarded with protons is shown in Fig. 7. A peak is observed at 76 kev which corresponds to a γ ray coming from the excitation of a level in Gd^{160}.

Tb^{159}

The lower panel in Fig. 5 shows the pulse-height spectrum when a Tb_2O_3 target is bombarded with 2.89-Mev protons. Peaks corresponding to γ rays of 77 kev and 167 kev are observed. In addition, a small rise in the curve at about 210 kev is also present. It is quite difficult to interpret this spectrum since the samples used in these experiments were most probably contaminated with other rare-earth materials. Furthermore, since the sample available to us consisted of $(NH_4)Tb(SO_4)_2$ the oxide had to be obtained by precipitation with NH_4OH. It is possible therefore that the high continuous background and perhaps some of the observed lines are due to light impurities. It should also be noted that both the K x-ray and the 77-kev lines are broader than the corresponding lines observed from europium. The width of the K x-ray line could be explained either by the existence of an energy level near this energy in Tb^{159} or—more likely—a rare-earth contamination in the target with a slightly larger Z

(probably Dy or Er). The latter explanation is also favored by the composite nature of the 77-kev line. (However, Huus *et al.*[18] and Jordan, Cork, and Burson[23] do find evidence for a low-energy transition in Tb^{159} so that the first explanation cannot be entirely excluded.) We have tentatively assumed that at least part of the 77-kev line and perhaps also the 167-kev line arises from the excitation of Tb^{159}. No cross sections for these lines are given because of the doubtful assignment.

IV. INTERPRETATION OF RESULTS

Table I shows a summary of the results for the isotopes discussed in the previous sections. The procedure to determine the radiative transition probability from the number of γ rays per proton listed in column 5 of Table I will now be outlined. The cross section for electric quadrupole excitation has been given by Alder and Winther.[24] If one uses the notations of their paper, the cross section is

$$\sigma(E2)=\frac{2\pi^2}{25}\frac{m_1^2v_f^2}{Z_2^2\hbar^2}B(E2)g_{E2}(\xi) \tag{1}$$
$$=\psi(E)B(E2),$$

where

$$\xi=\frac{Z_1Z_2e^2}{\hbar^2}\left[\frac{1}{v_f}-\frac{1}{v_i}\right]. \tag{2}$$

The definition of $B(E2)$ in Eq. (1) has been changed slightly from that used by Alder and Winther. Our $B(E2)$ is equal to their $B(E2)$ divided by e^2. The electric excitation cross section is related to the number of γ rays per proton emitted from a thick target (N_γ) by:

$$N_\gamma=\frac{N_Aa}{\alpha_T+1}\int_0^{E_p}\frac{\sigma(E2)}{S(E)}dE, \tag{3}$$

where N_A is the number of atoms per gram, a is the isotopic abundance of the material under investigation, $S(E)$ is the stopping power of the target material in Mev/(g/cm^2), α_T is the total internal conversion coefficient of the level and $\sigma(E2)$ is the electric excitation cross section given in Eq. (2). The upper limit of the integration is the initial energy of the proton. The electric excitation cross section is the product of two factors, one depending on proton energy and the dynamics of the collision [$\psi(E)$ in formula (1)] and the other depending only the radiative transition probability of the energy level under consideration [$B(E2)$ in formula (1)]. The quantity of interest is $B(E2)/(\alpha_T+1)$. Inserting (1) into (3) and solving for $B(E2)/(\alpha_T+1)$ gives

$$\frac{B(E_2)}{\alpha_T+1}=\frac{N_\gamma}{N_AaI(E_p)}, \tag{4}$$

where

$$I(E_p)=\int_0^{E_p}\frac{\psi(E)}{S(E)}dE. \tag{5}$$

Once N_γ is measured, the evaluation of the radiative transition probability depends upon the evaluation of (5). The functions $\psi(E)$ have been tabulated[25] for a wide range of values of proton energies. The stopping powers $S(E)$ for the various oxide targets were obtained from the experimental values for gold and oxygen given by Allison and Warshaw[26] by using interpolation procedures previously[27] described. The functions $\psi(E)/S(E)$ were then plotted against proton energy (E) and the numbers $I(E_p)$ were determined by graphical integration from these curves. The probable error introduced in the value of $B(E2)/(\alpha_T+1)$ by uncertainties in the value of the stopping power and by the interpolation procedure is of the order of 15%. The values of $B(E2)/(\alpha_T+1)$ are listed in column 6. The cumulative errors from the values in N_γ and from the integration of the stopping power make it probable that the absolute values of $B(E2)/(\alpha_T+1)$ quoted are reliable to roughly a factor of two. The relative values of the $B(E2)/(\alpha_T+1)$ in any series of isotopes which have roughly similar energy level schemes are very much more reliable (~15%).

In order to calculate the actual radiative transition probabilities, $B(E2)$, from the values of $B(E2)/(\alpha_T+1)$, values for the total internal conversion coefficient, α_T, must be obtained for each transition. Very little experimental data on the magnitudes of these coefficients exist in the literature, and hence it is necessary to use extrapolations of the rather inadequate theoretical values in the literature.[28–30] The methods used to calculate the values of α_T shown in column 7 of Table I are essentially similar to those used in our previous report[8] and those of Sunyar.[31] The errors in these estimated values are of course quite large, and therefore the values of $B(E2)$ and Q_0 (cross section) listed in Table I are order-of-magnitude estimates only and should not be used to draw quantitative theoretical conclusions. We have included these numbers in the table for two reasons:

(1) The trends in the values of $B(E2)$ in any series of isotopes are considered reliable enough for comparison with theory and are therefore of some interest.

(2) The values of Q_0 (energy) calculated from the energies of these transitions, assuming the validity of the "strong coupling" approximation, are all very sub-

[23] Jordan, Cork, and Burson, Phys. Rev. **92**, 315 (1953).
[24] K. Alder and A. Winther, Phys. Rev. **96**, 237 (1954).
[25] K. Alder and A. Winther (private communication).
[26] S. K. Allison and S. D. Warshaw, Revs. Modern Phys. **25**, 779 (1953).
[27] McClelland, Mark, and Goodman, Laboratory for Nuclear Science, Massachusetts Institute of Technology LNS-MIT Technical Report No. 66, 1954 (unpublished).
[28] Rose, Goertzel, Spinrad, Harr, and Strong, Phys. Rev. **83**, 79 (1951).
[29] Gellman, Griffith, and Stanley, Phys. Rev. **85**, 944 (1952).
[30] B. I. Spinrad, Phys. Rev. **98**, 1302 (1955).
[31] A. W. Sunyar, Phys. Rev. **98**, 653 (1955).

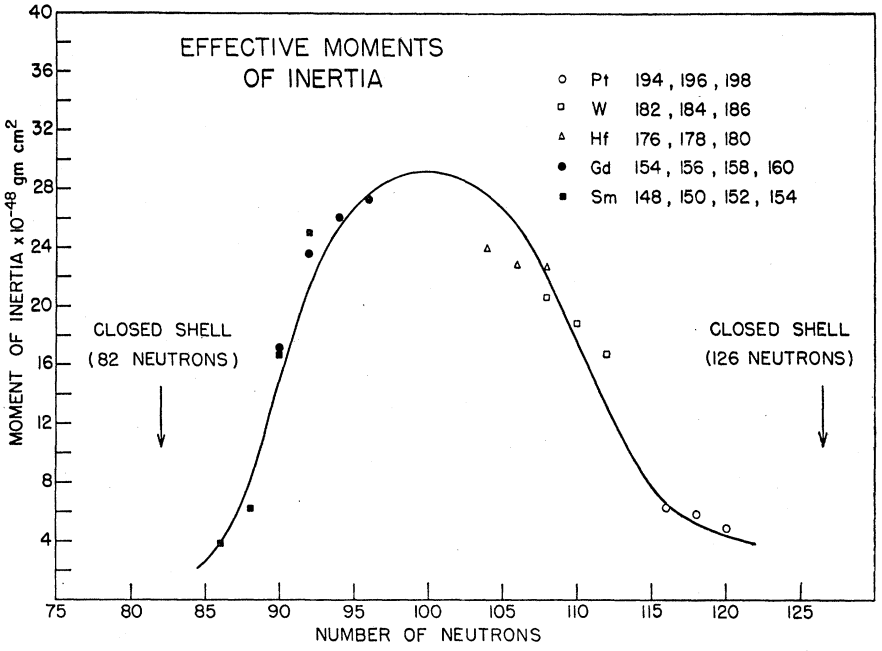

FIG. 8. Effective moments of inertia of even-A nuclei as a function of neutron number. The effective moment of inertia is calculated from the energy of the first excited level in each isotope by using the formula:

$$E=(\hbar^2/2\mathcal{I})I(I+1).$$

The trends exhibited by $\mathcal{I}$ are the same as those shown by known nuclear electric quadrupole moments. There is some doubt whether this formula is applicable for the observed levels in Sm^{148}, Sm^{150}, and the platinum isotopes.

stantially larger (outside experimental errors in either number) than those obtained from the cross sections—a fact which is also of some theoretical interest. (See reference 8.)

Several remarks regarding the experimental results are in order. The trends in the values of the energies and radiative transition probabilities for the even-A isotopes of gadolinium are in good agreement with the expectations of the "strong coupling" picture of Bohr and Mottelson.[5] The energies increase as the closed shell at 82 neutrons is approached while the transition probabilities decrease, which is a reflection of the fact that the largest intrinsic nuclear deformations are to be expected at a neutron number of about 96. It should be pointed out that the trends in the even-A isotopes of tungsten and hafnium[8,17] are the reverse of those observed in gadolinium because the closed shell at 126 neutrons apparently dominates their behavior.

The behavior of the even-A isotopes of samarium is more difficult to understand. In the neutron-rich isotopes Sm^{154} and Sm^{152}, the energies of the first excited levels are very close to those in the neighboring gadolinium isotopes, but in the isotopes Sm^{150} and Sm^{148} the energies are 3 and 5 times larger, respectively. It has been suggested[32] that, at this point in the periodic table, the "strong coupling" approximation breaks down and that the fast $E2$ transitions observed below this point are the "vibrational" levels predicted by the "weak coupling" approximation. A strong argument in favor of this interpretation is that the even-A nuclei below this point have second excited levels at roughly twice the energy of the first level which is what would be expected for vibrational spectra (see the summary of data in reference 32). Furthermore, in odd-A nuclei below this point in the periodic table, electric excitation experiments have not revealed a single case[9,33] where the first two energy levels fit into a good "strong coupling" (i.e., rotational) spectrum; whereas above this point many examples[2,8,17] of well-developed rotational spectra are known.

The odd-A isotopes, for which results are given in Table I, also show some interesting properties. The three low-energy γ rays observed from the europium target fit into the proper rotational sequence for a nucleus with ground level spin 5/2. These energy levels have been tentatively assigned to Eu^{153}. It is somewhat difficult to understand why the isotope Eu^{151} does not also exhibit a good rotational spectrum, since several examples of neighboring odd-A isotopes where both numbers have proper rotational spectra are in existence.[8,17] The energy levels observed in the odd-A isotopes of gadolinium also raise some interesting questions. The situation here should be roughly similar to the one encountered in the hafnium[8,17] isotopes where both the odd- and even-A isotopes have strongly excited first energy levels at roughly similar energies. In the case of the odd-A gadolinium isotopes the energy levels observed have transition probabilities which are of the order of 30 times smaller than those observed in the neighboring odd-A isotopes (see Fig. 3). Temmer and Heydenburg[17] have suggested that these γ rays arise from the second excited levels in these nuclei and actually have some evidence for the existence of energy levels in these isotopes at about 48 kev. This would

[32] G. Scharff-Goldhaber and J. Weneser, Phys. Rev. 98, 212 (1955).

[33] G. M. Temmer and N. P. Heydenburg, Phys. Rev. 98, 1308 (1955).

account for the low intensities of the observed lines. More work on these levels should be done to clear up this point.

The results of the electric excitation experiments which have been carried out by many workers in this field all serve as an excellent confirmation of the general features of the collective model. The existence of a great number of fast $E2$ transitions, the existence of well-defined rotational spectra, the probable existence of vibrational spectra, and the trends exhibited by the energies and the transition probabilities are all in agreement with the predictions of the model (see Fig. 8). There are, however, several important experimental results for which the model does not as yet provide any explanation. The effective moments of inertia of the rotational levels which have been identified are all larger by factors ranging from three to seven than those which are calculated from intrinsic nuclear deformations measured in other ways.[8,17,34] (That is, the energies of the observed rotational levels are too low by factors of ten to fifty.) The reason for the apparently sharp break between the regions in the periodic table where the "strong coupling" and the "weak coupling" approximations are applicable is also not well understood. Finally, if the energy levels which are observed in the "weak coupling" region are indeed "vibrational" levels, then their energies are also much lower[9,33] (factors of roughly ten) than those which would be expected from the crude hydrodynamical estimates worked out in Bohr and Mottelson.[5] The fact that both the "rotational" and "vibrational" levels apparently have energies which are smaller by roughly the same order of magnitude than those expected from the model suggests that a revision of the fundamental assumptions about either the nature of the nuclear "fluid" or its distribution in the nuclear volume may be necessary.

[34] K. W. Ford, Phys. Rev. **95**, 1250 (1954).

ACKNOWLEDGMENTS

The authors are indebted to Dr. C. P. Keim of the Oak Ridge National Laboratory for his very kind help in procuring the enriched isotopes, and to Professor L. C. Bradley of MIT for providing some of the samples of rare-earth oxides used in this work. We would like to thank Professor V. F. Weisskopf, Professor M. Deutsch, Professor S. D. Drell, Dr. Gertrude Scharff-Goldhaber, and Dr. G. Goldring for many useful conversations and for their continued interest in these experiments. We are grateful to many of our colleagues in this field for keeping us informed of their latest results, some of which were invaluable in the preparation of this report. Finally it is a pleasure to acknowledge the help of Mr. Matti K. Salomaa, who designed and built much of the electronic equipment and Mr. Allen Lenchek who performed many of the calculations.

PHYSICAL REVIEW VOLUME 100, NUMBER 3 NOVEMBER 1, 1955

Empirical Correlation of Nuclear Magnetic Moments

R. K. OSBORN AND E. D. KLEMA
Oak Ridge National Laboratory, Oak Ridge, Tennessee
(Received April 18, 1955)

A simple generalization of the extreme shell model, based upon the kinematics of the collective model, is proposed for the correlation of nuclear magnetic moments. It is shown that, if the concept of a rotating core is adjoined to that of the single-particle model, largely in disregard of dynamical considerations, then by the aid of three simple empirical rules ground-state wave functions may be easily constructed which correctly express the parities, spins, and magnetic moments of all nuclei for which $A \geqslant 7$, with the exception of W^{183}.

The choice of a particular set of empirical rules was dictated primarily by the twofold desire to keep their number to a minimum and at the same time restrict the consequent wave function to but two components; hence, considerable oversimplification of the true state of affairs is inevitable. However, the internal consistency of the results does point up strikingly the previously observed, but not explicitly investigated, possibility that the nature of the variable degrees of freedom required for generalization of the single-particle model may differ fundamentally for $j=l+1/2$ in contrast to $j=l-1/2$ single-particle configurations —being predominantly those of the core in the former instance and those of the single particle in the latter.

I. INTRODUCTION

THE single-particle model of the nucleus, which assumes that the relevant degrees of freedom required for a description of the nuclear ground state are those of the last odd particle (for even-even and odd-even nuclei, and hence no degrees of freedom for the former), leads to the well-known Schmidt values for magnetic moments. Presumably the deviations of the experimental moments from the Schmidt limits are to be accounted for through the interplay of some other degrees of freedom of the nuclear system than those of the last odd particle. One of three main lines of endeavor have usually been followed in the attempt to uncover the nature and significance of these extra degrees of freedom required for an understanding of nuclear ground-state properties.